Supporting Material

METHODS

Synthesis of amine-modified polyacrylamide nanoparticles Amine-modified polyacrylamide nanoparticles were synthesized by inverse-emulsion polymerization. An acrylamide solution (1.35 g acrylamide and 29 mg bis-acrylamide in 3.3 ml water) was polymerized in sodium bis-(2-ethyl-hexyl)sulfosuccinate (AOT) emulsifier solution (7.7 g AOT dissolved in 27.9 g toluene) by adding potassium persulfate (5.55 mg dissolved in 0.15 ml water) and gentle stirring for 10 min at 45°C. After polymerization, the toluene was evaporated at 50°C under reduced pressure. The polymerized particles were washed several times in methanol, dissolved in water, and lyophilized.

To add amine groups to the particles, ~40 mg of the lyophilized material was dissolved in anhydrous ethylenediamine (160 ml) and stirred at 75°C for various reaction times (1–7 hr, depending on the level of amination required). At the end of each reaction time, an aliquot of the solution (~30 ml) was separated from the bulk, cooled, and mixed with an equal volume of 1-butanol, to precipitate the particles. The precipitate was washed with methanol several times and finally dissolved in 0.5–1 ml of water.

Measurement of concentration and diameter of the particle using negative-stain electron microscopy Regular copper grids (Structure Prove Inc., West Chester PA) were coated with a thin carbon film (CADE; Meiwafosis Co., Osaka, Japan) and rendered hydrophilic by a plasma etcher (SEDE; Meiwafosis Co.). To accurately determine the concentration of particles in stock solution, we needed to make sure that no particles were lost during the sample preparation on an EM grid. For this purpose, the stock suspension of nanoparticles was diluted 100 times with unbuffered 1% uranyl acetate, and one microliter of this suspension was applied on a grid and air-dried without any blotting procedure.

To determine the average diameter of nanoparticles, a top view of the individual nanoparticles on the carbon film (Fig. 1 *A*) was fit to ellipsoids, and the major and minor axes of each ellipsoid were measured. As their aspect ratio of 1.13 ± 0.13 (n = 865) indicates that the particles are almost round, the diameter of each particle was calculated by averaging the major and minor axes. The average diameter of the particles (62 ± 14 nm), obtained from top view, was further corrected for a flattening effect, due to the adsorption of the particle to the charged surface of the carbon film and the air-drying of the negative-stain. The correction was made based on a side view of the particles that were accidentally observed along the curved surface of the torn carbon film (Fig. S1). The average diameter of the particle d was finally calculated as 57 ± 13 nm ($d^3 = 62^3/1.27$), from the ratio of equatorial radius to height, 1.27 ± 0.16 (n = 11).

Estimation of particle diameter under dark-field microscopy When the motions of the particles were analyzed by DFM, the sizes of the particles were estimated from their light scattering intensities using the following procedure. Initially, we measured the light intensities of the particles, $I_{p(0)}$, that were firmly attached to the glass surface under the DFM (Fig. S2 *A–D*). According to the theory of Rayleigh scattering (1), the intensity of the light scattered by a particle $I_{p(0)}$ is expected be proportional to the sixth power of its

diameter *d* (light absorption by particle can be ignored, since the diameter of the particle is < 1/15th the wavelength of light). Thus, we regarded the parameter $I_{p(0)}^{1/6}$ as a measure of particle diameter, and compared its distribution with the distribution of diameter directly measured by TEM, *d* (Fig. S2 *E, F*). The results reveal that these two distributions do not coincide because DFM cannot detect objects smaller than a certain size (2). When the same stock of particle suspension was diluted and the number of particles attached to the carbon film/glass surface was counted by both TEM and DFM, approximately 70% of the particle densities measured by TEM were detected by DFM. To correlate the distributions of *d* and $I_{p(0)}^{1/6}$, we plotted a cumulative frequency distribution of the particle diameters, either in the form of *d* or $I_{p(0)}^{1/6}$ (Fig. S2 *G*). These two curves were best superimposed when we assume $d = 22.5 \times I_{p(0)}^{1/6}$ (in nm), indicating that the minimum diameter of a particle detectable by our DFM is ~40 nm.

Next, for a particle bound/moving along an MT, the light intensity of the MT I_{MT} was first subtracted from the light intensity of the particle on the MT, $I_{p(\mathrm{MT})}$, and the residual intensity was converted to diameter using the foregoing equation. Admittedly, this is a rough approximation, as optical interference between the particle and the MT is very complicated (1) and taking this effect into consideration would require a lot more time and effort. From an independent experiment, the error in the particle diameter incurred by our approximation was estimated to be ±20% maximally. More importantly, even if our estimation includes 20% error, it does not ultimately alter the relative values of *Q* for this series of particles with varying amine densities, as shown in Fig. 3.

Estimation of viscous drag near MT surface The free diffusion constant D_0 of a particle with a radius *a* in solution with viscosity μ can be calculated using the Einstein-Smoluchowski relation $D_0 = k_{\mathrm{B}}T/f_0$, where $f_0 = 6\pi\mu a$. Near the glass surface, free diffusion of a particle slows down, because the viscous drag on a particle, *f*, increases in proximity to the planar surface (3). The drag is expected to be higher than that on a particle in solution by a factor of r ($= f/f_0$) defined as:

$$r = \frac{1}{1-(9/16)(a/l)+(1/8)(a/l)^3-(45/256)(a/l)^4-(1/16)(a/l)^5},$$

where *l* is the distance between the center of the particle and the glass surface.

For nanoparticles moving along the MT, which is attached to the glass surface, the situation is more complex; in this case, the viscous drag on the particle may increase due to the wall effect from both the glass surface and the surface of the MT. As the calculation of a factor *r* for such a case is highly complicated, we approximated the range of *r* as follows: as the center of a particle ($2a = 59$ nm) moving along the MT (diameter = 25 nm) is at a distance $25 + 59/2 = 54.5$ nm from the glass surface ($= l$), if we ignore the wall effect due to the MT, *r* is expected to be 1.4. On the other hand, if we assume that the particle is moving in proximity to the glass surface, *r* is expected to be 3.1 ($a = l = 59/2$). The real number for *r* may be somewhere between 1.4 and 3.1. Based on this estimation, the free diffusion constant of a particle in proximity to the MT filament, without electrostatic or any other

constraint from the surface, is expected to be 2.4–5.2 $\mu m^2/s$.

For a KIF1A molecule moving along MT, we used $r = 3.1$, obtained by assuming the diameter of KIF1A ~5 nm and assuming MT as a plane wall.

REFERENCES

1. van de Hulst, H. C. 1981. Light Scattering by Small Particles. Dover Publications, Inc., New York. 63-102.
2. Mizushima, Y. 1988. Detectivity limit of very small objects by video-enhanced microscopy. Applied Optics 27:2587-2594.
3. Happel, J., and H. Brenner. 1973. Low Reynolds Number Hydrodynamics. Martinus Nijhoff, The Hague. 322–331.

TABLE S1 Concentration of particles applied to the flow cell in each experiment

ρ [nm^{-3}]	Q	Particle concentration [/μl]	
		Binding assay*	Analysis of movement†
0.30	13	4.8×10^7	3.2×10^7
0.36	15	1.5×10^7	6.1×10^6
0.55	24	4.7×10^6	4.1×10^5
0.59	26	1.6×10^6	1.5×10^5
0.73	32	1.5×10^6	1.6×10^5
0.96	42	1.5×10^6	1.1×10^5

* Results are shown in Fig. 2 *A*.

† Results are shown in Figs. 2 *B–D* and Fig. 3.

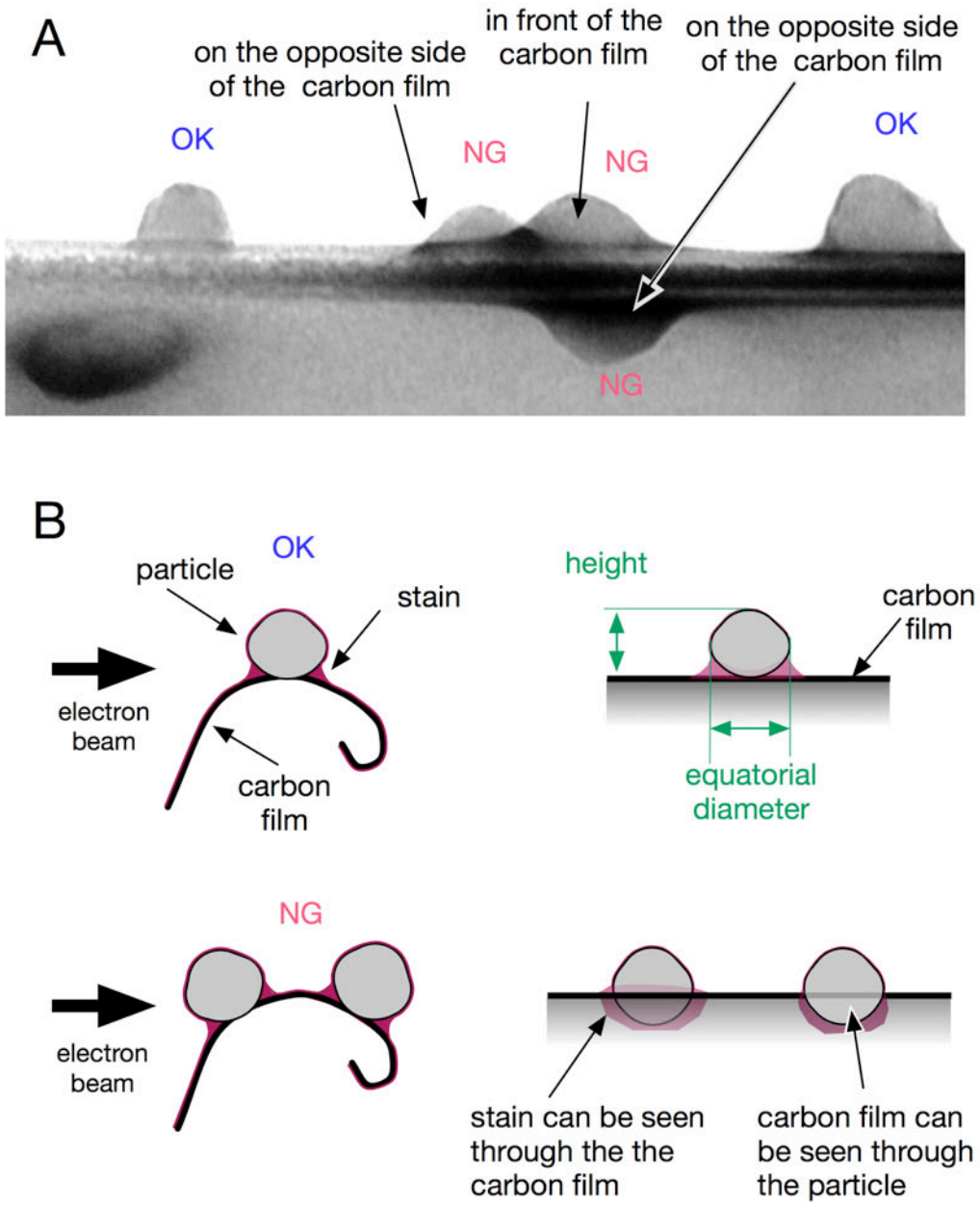

FIGURE S1 Analysis of the particle flattening by negative-stain electron microscopy. (A) Negative-stained EM images of the nanoparticles attached along the ridge of the torn and curved carbon film. (B) Schematic drawing explaining the relation between the orientation of the particles on the carbon film (left) and their EM images (right). Among those nanoparticles on the curved film, only those particles positioned along the ridge of the curved carbon film were analyzed (indicated by "OK") and those particles either in front of or behind the curved ridge were excluded from the analysis (indicated by "NG"). As both particles and carbon film were semitransparent to the electron beam, it was easy to distinguish between these two cases. For the particles judged as "OK", the ratio of equatorial radius to the height, a measure of flattening, was thus calculated to be 1.27 ± 0.16 (n = 11).

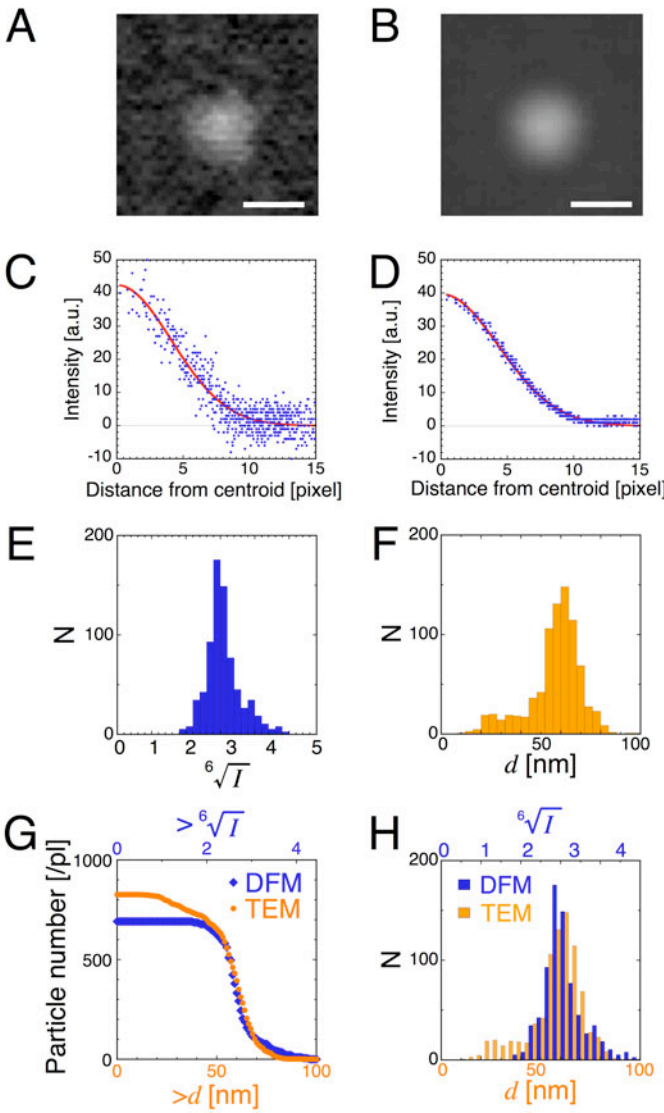

FIGURE S2 Determination of particle size by dark-field microscopy. (*A*) A single video-frame image (33 ms exposure) of a particle firmly attached to a glass surface. (*B*) Video images of the same particle averaged for a total of 1 s (i.e., 30 video frames). Bar = 12 pixels (0.5 μm). (*C, D*) For the images shown in *A* and *B*, the light intensity of each pixel $I(r_c)$ was plotted as a function of the distance from the centroid, r_c, in *C* and *D*, respectively. After subtraction of the background intensity, the distribution showed good fit to the Gaussian function (red lines). The intensity of the particle $I_{p(0)}$ was calculated by integrating the Gaussian function. The distributions of the particles with different diameters can be fitted to the Gaussian functions with same number for SD, which indicates that the distribution represents the point-spread function of the microscope. (*E*) The distribution of $I_{p(0)}^{1/6}$ measured for 277 particles. (*F*) The distribution of the diameters measured by TEM; in total, 865 particles were measured. (*G*) Cumulative frequency distributions of $I_{p(0)}^{1/6}$ and d; the fraction of particles with diameter equal to or larger than a given $I_{p(0)}^{1/6}$ or d versus the $I_{p(0)}^{1/6}$ or d is shown, respectively. The particle concentrations were converted to those in the original stock solution, taking into account the dilution factor. The two curves are optimally superimposed when $d = 22.5 \times I_{p(0)}^{1/6}$. These results imply that the minimum diameter of a particle detectable by DFM is ~40 nm. (*H*) The two histograms shown in (*E*) and (*F*) are plotted in one figure, using the same conversion ratio as in (*G*).

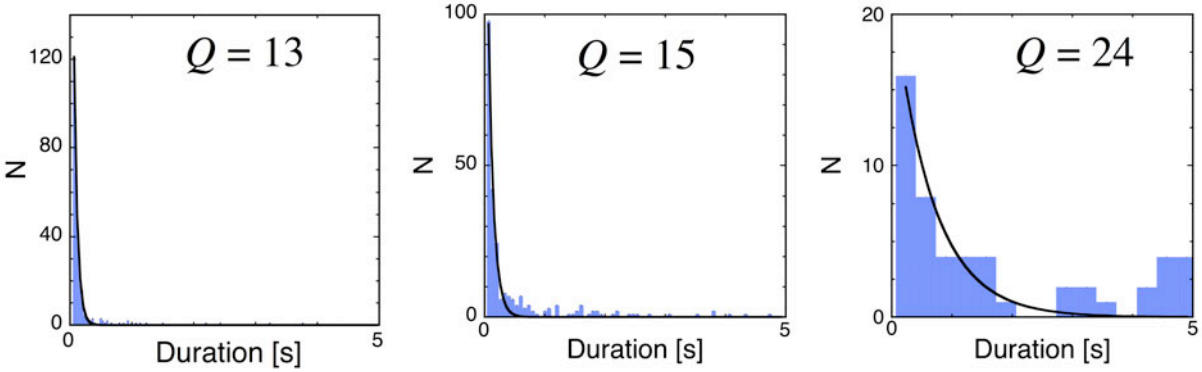

FIGURE S3 The duration of interaction for charged particles with various number of effective charges, Q. Durations of interaction shorter than 0.067 s (two video frames) were excluded. Each dataset was fitted to an exponential curve with decay constant of 0.055, 0.088, and 0.66 s for particles with Q (from left to right) of 13, 15, and 24, respectively.